DYNA
ISSN: 0012-7353
Universidad Nacional de Colombia

Dorado-Bustamante, Kevin; Leal-Marin, Sara; Estupiñán-Duran, Hugo
Electrochemical analysis of the degradation of nitrided zirconia 3Y-TZP
DYNA, vol. 85, no. 206, 2018, July-September, pp. 9-15
Universidad Nacional de Colombia

DOI: https://doi.org/10.15446/dyna.v85n206.68296

UNIVERSIDAD NACIONAL DE COLOMBIA
SEDE MEDELLÍN
FACULTAD DE MINAS

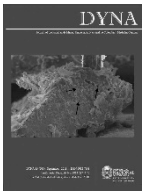

DYNA
http://dyna.medellin.unal.edu.co/

Electrochemical analysis of the degradation of nitrided zirconia 3Y-TZP

Kevin Dorado-Bustamante [a], Sara Leal-Marin [b] & Hugo Estupiñán-Duran [b]

[a] *Departamento de Física Nuclear, Instituto Balseiro, San Carlos de Bariloche, Argentina. kadoradob@gmail.com*
[b] *Grupo de tribología y superficies, Facultad de Minas, Universidad Nacional de Colombia, Medellín, Colombia. slealma@unal.edu.co, haestupinand@unal.edu.co*

Received: October 14th, 2017. Received in revised form: March 2nd, 2018. Accepted: March 20th, 2018

Abstract
Zirconia is a material that is susceptible to changes in its structure from the tetragonal to the monoclinic phase caused by variations in temperature or by contact with water. One way of achieving the stability of the tetragonal phase at low temperatures is by incorporating anionic gaps in its crystal lattice through doping procedures with aliovalent anions such as nitrogen. Nitrogen replaces the oxygen in the crystal lattice, which stabilizes the tetragonal structure of zirconia at low temperatures. The aim of this research was to evaluate the degradation of nitrided zirconia 3Y-TZP after it was immersed in artificial saliva for 0, 7, 14, and 21 days. Interfacial processes such as oxide-formation were assessed simultaneously using the electrochemical impedance spectroscopy test. Additionally, morphological, topographic, and composition changes were analyzed in the degradation process using SEM-EDS and AFM.

Keywords: 3Y-TZP; nitriding; aging; artificial saliva; EIS.

Análisis electroquímico de la degradación de circonia 3Y-TZP nitrurada

Resumen
La circonia es un material susceptible a cambios en su estructura de la fase tetragonal a monoclínica, ocasionados por cambios en la temperatura o contacto con agua. Una manera de alcanzar la estabilidad de la fase tetragonal a bajas temperaturas es a través de la incorporación de vacancias aniónicas en su estructura cristalina por medio de procedimientos de dopado con aniones aliovalentes como el nitrógeno. El nitrógeno reemplaza el oxígeno en la estructura cristalina y estabiliza la estructura tetragonal de la circonia a bajas temperaturas. El objetivo de este trabajo fue evaluar la degradación de la circonia 3Y-TZP nitrurada a través de su inmersión en saliva artificial por 0, 7,14 y 21 días, evaluando los procesos interfaciales como la formación de óxidos a través de espectroscopia por impedancia electroquímica. Adicionalmente se analizó la morfología, topografía y cambios de composición en el proceso de degradación empleando SEM-EDS y AFM.

Palabras clave: 3Y-TZP; nitruración; envejecimiento; saliva artificial; EIE.

1. Introduction

The development of materials in the biomedical field has positioned zirconia as a material that has an increasing number of applications due to its mechanical and biocompatibility properties [1, 2]. However, zirconia under conditions of mechanical loads exhibits slight increases in temperature and a tendency to present structural changes transforming its crystalline structure from a monocyclic to a tetragonal phase. This phase change generates a 3-4% thermal expansion, producing cracks and degradation or material failure [3], and mechanical properties are decreased [4]. In addition, contact with body fluids containing aggressive ions generates phase transformation even after short periods of time [4]. For these reasons, in the zirconia sintering process, it is convenient to add stabilizing oxides to maintain the tetragonal

How to cite: Dorado-Bustamante, K., Leal-Marin, S. and Estupiñán-Duran, H., Electrochemical analysis of the degradation of nitrided zirconia 3Y-TZP. DYNA, 85(206), pp. 9-15, September, 2018.

structure of the zirconia at room temperature: common aggregated oxides are Yttrium Oxide (Y_2O_3), calcium oxide (CaO), and magnesium oxide (MgO) [5, 6].

The tetragonal polycrystalline zirconia stabilized with 3% mol yttria (3Y-TZP) is one of the ceramics that has been used increasingly in use in dental applications for prostheses, crowns, and implant pillars [2, 7-8]. Nonetheless, in some biomedical applications, the addition of oxides is not enough to obtain adequate degradation resistance. For this reason, this paper explores the ionic nitriding process to improve the mechanical properties and resistance to material degradation in body fluids. In the nitriding process, the inclusion of nitrogen with plasma generates a substitution for anionic vacancies replacing the oxygen with nitrogen in the crystalline lattice to stabilize the surface of the material [9]. Usually, these processes are carried out in ovens at temperatures between 1400 °C and 1900 °C in nitrogen atmospheres for between 2 and 12 hours. However, at 1170 °C there is a phase change in the crystalline structure from monoclinic to tetragonal. This change in the structure of the zirconia affects the material, and there is a consequent deterioration degradation resistance [9-11].

Aging processes are typically characterized by autoclaving at 134°C at a pressure of 200 kPa for approximately 1 h; this may correspond to the material at body temperature aging four years [12-13]. During these processes, the initial state and the final state are evaluated, without considering the deterioration in short periods of time and without following a step by step process of the consequent formation of unstable oxides. Electrochemical impedance spectroscopy is a technique that allows the degradation phenomena that occur in a material exposed to a fluid to be evaluated and the changes in material integrity to be monitored as well as the incidence of the fluid and the formation of oxides or degradation products [14].

The objective of this study was to evaluate the resistance to deterioration of 3Y-TZP samples that have been treated with three different plasma nitriding temperatures (450 °C, 480 °C, and 520 °C). These were used in this research as nitriding temperatures in order to avoid monoclinic transformation and to induce a surface modification with the formation of a semi-crystalline zirconia oxide that increases protection against physiological fluids without the mechanical properties significantly being affected [12, 15]. An experimental setup was performed keeping zirconia samples that were both treated (nitriding) and untreated immersed in an artificial saliva saline solution type Afnor [16] for 21 days. The degradation behavior was evaluated in 7-day intervals using the electrochemical impedance spectroscopy technique. At the same time, other techniques were used to characterize the samples, such as scanning electron microscopy and atomic force microscopy to evaluate the morphology and changes in roughness occasioned with the aging of the material.

2. Materials and methods

2.1. Sample preparation

Pre-sintered 3Y-TZP powder compact blocks with 87-95%ZrO_2, 3-6% Y_2O_3, 1-5% HfO_2, and 1% Al_2O_3 compositions were used. These blocks were sectioned with a microcutter at 250rpm (Isomet 100, Buehler) to obtain samples that were 15x15mm and 2mm thick. Samples were then sintered in a furnace (Ceramill therm®, Armann Girrbach) at 1450 °C for 10 hours using an 8 °C/min heating ramp and then cooled to room temperature. After this process, the surfaces of the samples were polished with silicon carbide sandpaper # 340, 400, 600, and 1200 following the ASTM E3-01 standard. They were rinsed with distilled water, sonicated in isopropyl alcohol, and then dried at room temperature before the nitriding process.

2.2. Nitriding process

The ionic nitriding of the 3Y-TZP zirconia samples was performed at three temperatures (450, 480, and 520 °C) in an industrial furnace using a pulsed direct current. Each temperature was maintained for 2h with a vacuum of 3 Pa, a pressure of 400 Pa, and a 75/25 mixture of H_2/N_2. After the nitriding process was completed, the samples were cooled in the oven to an ambient temperature under a nitrogen atmosphere.

2.3. Immersion in saline solution

The degradation of the samples treated and untreated (NT) was evaluated after immersing the samples for 21 days in plastic sealed containers with an artificial saliva saline solution type Afnor [16]. The composition of this is shown in Table 1; it was prepared in 250mL of distilled water and had a pH of 6.55. All the reagents employed were analytical reagent grade.

2.4. Morphological and compositional analysis

2.4.1. Scanning Electron Microscopy (SEM) - Energy Dispersive X-Ray Spectroscopy (EDS)

The morphological identification was performed using SEM equipment (EVO MA10, Carl Zeiss) and the EDS compositional analysis was performed with an X-Act detector (Oxford Instruments). There was a 10kV acceleration voltage, the composition data was obtained in areas (50*50 µm) by triplicate for each sample, and an average was also reported. During the observation, the samples were covered with a layer of gold.

Table 1.
Chemical composition Afnor artificial saliva

Reagent	Name	Amount (g/250ml)
NaCl	Sodium chloride	0.17
KCl	Potassium chloride	0.30
$NaHCO_3$	Sodium hydrogen carbonate	0.37
KSCN	Potassium Thiocyanate	0.08
$Na_2HPO_4*2H_20$	Disodium phosphate dihydrate	0.06
$CO(NH_2)_2$	Urea	0.32

Source: The authors.

2.4.2. Atomic force microscopy (AFM)

The topographical analysis was assessed using AFM (NX10, Park Systems) equipment in contact mode. Mappings of 10 x 10 µm were performed with a scanning rate of 1 Hz. Topographic images were obtained with a tip (NSC14, Mikromasch) that was 5 N/m, a constant force, and had a 160 kHz resonance frequency. For the height images obtained, the roughness factor Ra was defined as the average arithmetic roughness.

2.5. Electrochemical Impedance Spectroscopy (EIS)

The Electrochemical Impedance Spectroscopy (EIS) and Mott-Schottky (M-S) tests were carried out in a Potentiostat/Galvanostat (Interface 1000®, Gamry instruments) using a three-electrode electrochemical cell. A 99% purity graphite bar was used as a counter electrode, an Ag/AgCl electrode was used as a reference, and the 3Y-TZP (treated and untreated) was used as the working electrode. An artificial saliva type Afnor saline solution was used as the electrolyte. The tests were carried out at body temperature (37 °C) using a thermostat bath (E100, LAUDA) connected to the electrochemical cell with an external circuit. The EIS tests were obtained with a 70 mV amplitude in a frequency range of 100 kHz to 0.01 Hz. The tests were undertaken before starting the immersion process (0 days) and then consecutively every 7 days until the 21-day immersion period was completed. The equivalent circuits proposed to adjust the Bode diagrams were carried out using the software Zview®.

3. Results and discussion

3.1. Morphological and compositional analysis

3.1.1. SEM and EDS

The elemental compositional analysis obtained by EDS (on the polished surface of the sample) was undertaken to identify the presence of nitrogen on the surface; it showed an increase in the percentage of this element with the nitriding treatment. Table 2 shows the results of the elemental composition. Besides nitrogen, elements such as yttria, hafnium, and zirconia (presented as elemental components of the compacted zirconia powders) were identified in all the samples. The additional presence of oxygen may be related to the formation of oxides during the nitriding process.

According to the data in Table 2, it can be seen that the oxygen concentration tends to decrease in all the proposed nitriding treatments, and there is an increase the nitrogen composition. Also, the O/N ratio was lower in the nitriding treatment at 450 °C and higher at 520 °C. The ratio obtained for 520 °C was very close to the untreated sample. This tendency may be related to the phenomenon of oxygen displacement by the nitrogen in the structure of the zirconia, which has already been reported by other authors [9]. Fig. 1 presents the morphological analysis of 3Y-TZP samples with and without nitriding treatment. In these images, no significant differences were observed between treated and untreated samples before immersion. Thus, the nitriding process did not affect the structure of the material in a macroscopic manner since the maximum temperature used was less than the temperature required for the monoclinic phase change of the zirconia (established at 1170 °C) [17]. The morphology observed was similar to other studies that have stabilized zirconia with 3% mol yttria [18].

Table 2.
Elemental composition of different samples

%Atomic	N K	O K	Y L	Zr L	Hf L	O/N
No treatment	2.91	64.76	0.66	31.31	0.37	22.25
450°C	4.03	61.39	0.60	33.39	0.35	15.23
480°C	3.19	63.70	0.90	32.39	0.31	19.96
520°C	2.99	63.11	0.82	33.42	0.38	21.11

Source: The authors.

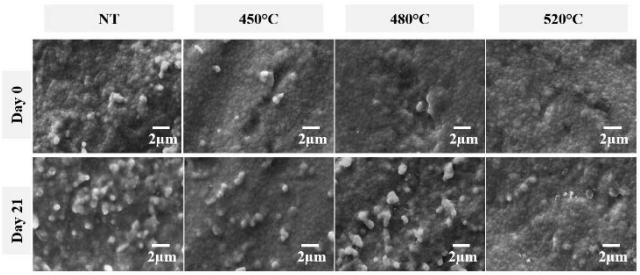

Figure 1. Secondary electron micrographs of samples subjected to different nitriding temperatures: before immersion in artificial saliva and after 21 days of immersion.
Source: The authors.

After being immersed for 21 days in the saline solution, samples revealed morphological changes associated with the degradation of the ceramic structure, they also had rounded particles and more visible bonding interfaces. Additionally Fig. 1 shows a great number of particles with irregular shapes that are observed as whiter areas (day 21); these were generated due to deposition of salts on the surface. However, the quantity of salt accumulation was lower than the detection limited by the EDS technique, thus, the presence of elements such as phosphorus, sodium, or chlorine was not detected. A clear difference between the treated and untreated samples was observed in the morphology of the ceramic aggregation particles. Using the formation of grains in the ceramic with the aggregation of particles as a reference, the untreated grains in the sample (NT) were a round shape and the grains in the nitriding samples were an ovoid elongated shape with fewer spaces between the particles. This phenomenon could be due to the presence of amorphous or semi-crystalline oxides, which were formed mainly in the lower energy zones of the ceramic bonding particles. Specifically, they occupied the spaces left by the bonding interlayers. The presence of this type of oxide has been corroborated with the results and analysis of the electrochemical impedance spectra obtained, especially after being immersed for 21 days in an artificial saliva electrolytic solution. After being immersed for 21 days in saline, there were no defects or cracks in the nitrided samples, as would be expected in unstabilized zirconia on contact with water, in which the tetragonal phase changes to the monoclinic phase [19].

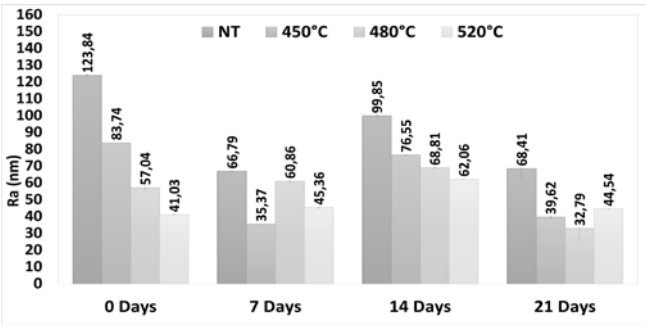

Figure 2. Results of roughness (Ra) for the samples that were immersed in artificial saliva.
Source: The authors.

3.1.2. AFM

The samples were observed using atomic force microscopy, and the topography and roughness are presented in Fig. 2 (samples were analyzed without polishing). The roughness values decreased as the nitriding temperature increased, which confirmed the SEM observations of probable formation of amorphous oxides in the interlayer sites of the bonding particles in the ceramic with nitriding treatment. This increased with the treatment temperature.

In general, from 0 to 21 days immersion in saline, the roughness values decreased 44.76% in the NT sample, and 52.68% and 42.51% in the samples nitriding at 450 °C and 480 °C, respectively. The roughness in the sample at 520 °C, increased to 8.55% at 21 days. The trend in intermediate immersion times (7 and 14 days) represented a drastic decrease in roughness in all samples (less in 480° C) at 7 days, with an increase at 14 days, and then a decrease at 21 days. This trend could be influenced by the occurrence of two simultaneous processes: a) the formation of amorphous oxides that result from the interaction of the ceramics with the aqueous saline solution, and b) the degradation of oxides and particles that are formed in the consolidation and nitriding process. These changes may be related with salt deposition in the surface. In this context, it is notable that the sample that presents the highest percentage of decrease in roughness was the sample with the highest nitrogen content (450 °C), and the sample with the lowest reduction in roughness was the one with the lowest nitrogen content (520 °C). This means that a relationship was established between the nitrogen content added and the increase in the affinity of bonding with either the oxygen presented in the thermal treatment or the aqueous medium for the formation of amorphous oxides. In addition to the changes presented in the roughness value, Fig. 3 shows that there were no notable topographic changes identified.

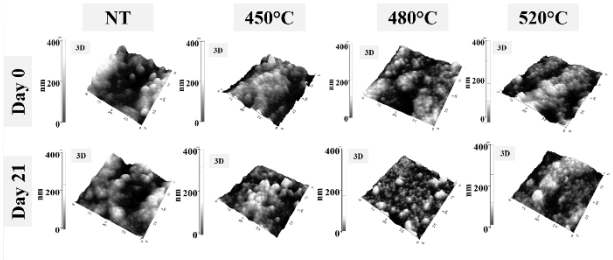

Figure 3. AFM images for the different samples at 0 and 21 days immersion
Source: The authors

Fig. 3 shows structures with robust grains that are more agglomerated in the samples that have been treated at 0 days as well as the structures with small grains and irregular forms at 21 days. This indicates uniform degradation or dissolution of the formed oxides during the nitriding process.

3.2. Electrochemical impedance spectroscopy analysis

The electrochemical test revealed parametric information related to the appearance of oxides that formed on the surface of the nitrided 3Y-TZP samples and the respective defects of these oxides that compromise the integrity of the material. Fig. 4 shows the spectra obtained for each sample both with no treatment and nitriding treatment at 0, 7, 14, and 21 days immersion in saline solution. In the untreated sample, particularly capacitive behavior was initially identified over a large range of frequencies with a wide loop in the phase angle vs. a frequency that was close to 90 degrees. The amplitude of the loop in the frequency range provides an idea of the stability of the sample. The resistance of this material at 0 days was approximately 1010 ohms. The 7, 14 and 21-day spectra showed patterns of untreated zirconia decay with the appearance of RC-transfer relaxations that were related to the formation of amorphous oxides with capacitive behaviors (high frequencies) and resistive behavior between the bulk of the material and these oxides (below 10 Hz). The loops of the phase angle graphs with an increased number of days immersed moved towards the high-frequency region; they became less ample, which is an indication of electrochemical instability due to the formation of amorphous oxides. The maximum deterioration of this sample was observed at 14 days immersion. It then recovered at 21 days until it reached an electrochemical resistance of 108 ohms. The presence of a capacitive region in this sample at 21 days between 0.1 Hz and 10 Hz becomes evident, and it is related to the involvement of the bulk of the zirconia under the action of the saline solution. The resistive behavior observed in this sample at 7 days immersion is part of a cycle of protection and deterioration of the sample due to the formation and dissolution of amorphous oxides and the penetration of aggressive electrolyte species from surface level to the bulk of the material.

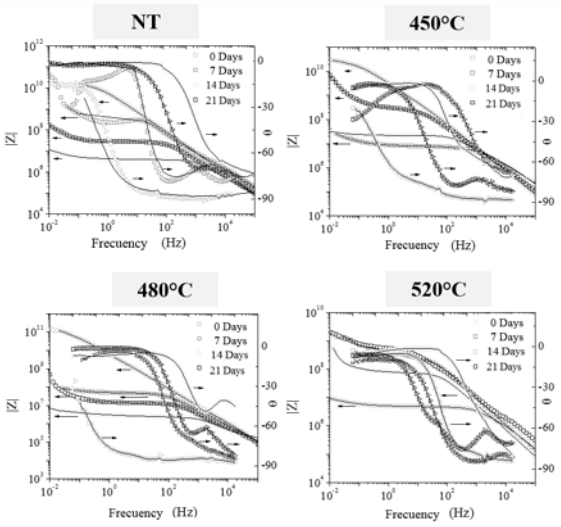

Figure 4. Bode diagrams for nitriding samples at different temperatures.
Source: The authors

The spectra of the samples with nitriding treatment behaved similarly to a sample without nitriding. The electrochemical resistance and stability were the highest at 0 days in the nitrided sample at 480 °C (1011 ohms), followed by the sample treated at 450 °C, which showed a slightly higher resistance in comparison to the untreated sample. The sample treated at 520 °C showed an approximate electrochemical resistance of 10:9 a lower value compared to the resistance of the other samples treated and without nitriding. The highest stability was observed in the sample treated at 480 °C because of its phase angle value in the spectrum which had a constant value of about 90 ° from 1 Hz to more than 10 kHz. With the variation of the residence time, behavior such as that of a sample without nitriding was observed. However, a higher electrochemical resistance was obtained at 21 days in comparison to the untreated sample. The sample nitriding at 520 °C presented an increase in its electrochemical resistance after 21 days in saline solution.

As shown in Fig. 5, for the quantitative analysis of the spectra obtained from the zirconia samples with and without immersion and treated and untreated, two equivalent electrical circuits were proposed. The RC components are related to charge transfer relaxations of the reactions that occur in the interfaces formed from the bulk of the material to the surface. The quantitative determination of the electrical parameters of these models was undertaken by adjusting the experimental parameters with those of the proposed model. Iterations in the software Z-view® were used for impedance analysis until a quantifiable error in four-digit chi-square decimals was found.

The proposed model (Fig. 5b) consists of an element representing the resistance of the artificial saliva (Rsa) used in series with an RC circuit (CPE1-R1), which represents the electrolyte/surface interface of amorphous zirconia formed on samples after 7, 14, and 21 days immersion in artificial solution. This oxidation is a product of the exchange of ions between the electrolyte and the substrate in parallel with a pair of RC elements (CPE2-R2), which represent the interface between the amorphous oxide formed and a zirconia oxide layer generated with the nitriding and the heat treatments. These elements are presented in series with a pair of RC (CPE3-R3) that represents the interface between zirconia samples both treated and untreated. The other model (Fig. 5a) was adjusted for all samples before being immersed in saliva due to the absence of amorphous oxide, which is represented in Bode diagrams with a simpler spectral morphology (Fig. 4).

Pure capacitances in the proposed circuits were replaced by constant phase elements to represent the inhomogeneities of the interfaces showing the formation of an oxide layer with nitriding and the presence of an amorphous zirconia oxide layer. Based on the proposed equivalent circuits, adjustment curves were presented which are shown in Fig. 4 as continuous lines that are superimposed on the dotted lines of the experimental data of the spectra. Table 3 shows the adjustment parameters of these curves for the different elements described.

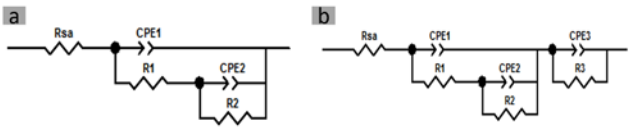

Figure 5. Equivalent circuit models a) at 0 days immersion, b) at 7, 14, and 21 days immersion.
Source: The authors

The CPE1-P values (immersion electrolyte/zirconium oxide) varied very little in a range between 0.8 and 0.9; this means that the hydrolytic degradation of the ceramic could be due to an increase in porosity due to disruption or dissolution of the anionic or cationic elements contained in the 3Y-TPZ. This is caused by oxygen product displacement of the hydrolysis to a local acid pH where reduction is generated and the structure goes through an aging process [20].

The phase values of the CPE1-P capacitance are reduced when immersion takes place, which is related to the formation of defects and porosities in the outermost layer of the zirconia samples. At the same time, the degradation of all samples is reflected in the behavioral changes in the frequency range: approximately between 1 Hz and 1 kHz. In this range, the electrochemical processes refer to the bulk transfer of the material.

The CPE2-P values that represent the transfer of charge restrictions at the interface between amorphous zirconia and nitrided zirconia remained within a range of 0.8 to 0.9. These values represent high integration between both oxides. The smaller CP3-T capacitance values were reached in the nitrided samples, especially in the sample treated at 450 °C which presented the highest impedance value. Moreover, the CPE3-P values showed a clear difference between the treated samples. Lower values in the nitrided samples could be related to the creation of vacancies of anions that generate homogeneities to the transfer of charge. Accordingly, the corresponding effect of an oxygen substitution by nitrogen is characterized by the formation of vacancies of additional anions, as per eq. (1) [9].

$$N_2\ (\text{Gas}) + 3O_x\text{O}\ (\text{YSZ}) = 2\text{NO'}\ (\text{YSZ}) + \text{V''O} + 3/2O_2\ (\text{Gas}) \quad (1)$$

In general, the substitution of oxygen ions for nitrogen ions help to stabilize the structure because of improvement in the concentration of oxygen vacancies (V"O). It has been found that YSZ zirconia with nitrogen doping is an excellent ionic conductor in cubic and tetragonal structures that even showed conductivity of nitrogen ions at high temperatures [9]. Lerch et al. demonstrated that the substitution of the anion (nitrogen) in ZrO2 or Yttrium-doped tetragonal zirconia (Y-TZP) stabilizes the cubic structure and improves the transport properties of these materials [21]. As reported by Cheng and Thompson, it is also possible to nitrate zirconia doped with yttria [22]. The stabilizing effects of both types of dopants are additive. Depending on the proportion of yttria/nitrogen incorporated, the materials show different types of structures with randomly

Table 3.
Adjustment parameters equivalent circuit models a) at 0 days of immersion, b) at 7, 14 and 21 days of immersion.

Immersion time	T (°C)	Rs (Ωcm^2)	R1 (Ωcm^2)	CPE1-T (F/cm^2)	CPE1-P	R2 (Ωcm^2)	CPE2-T (F/cm^2)	CPE 2-P	R3 (Ωcm^2)	CPE3-T (F/cm^2)	CPE 3-P	χ^2 (E^{-4})
0 days	**NT**	5665	2.00E9	2.22E-11	0.97	1.41E10	1.32E-11	0.63	-	-	-	9.78
	450	402	5.29E8	2.76E-11	0.97	3.50E10	4.72E-11	0.64	-	-	-	9.60
	480	4560	2.33E10	2.67E-11	0.94	2.25E11	9.23E-12	0.51	-	-	-	19.23
	520	3927	7.304E7	5.96E-11	0.91	9.438E7	2.15E-8	0.6	-	-	-	11.94
7 days	**NT**	45278	8.18E6	1.73E-11	0.94	3.089E8	9.71E-12	0.99	1.88E9	7.82E-9	0.99	19.35
	450	18372	1.04E9	9.22E-11	0.80	1.03E9	6.13E-15	0.51	7.42E7	1.88E-7	0.55	59.4
	480	17060	-8.63E10	9.09E-11	0.86	8.64E10	5.46E-17	0.99	2.04E7	5.26E-8	0.76	28.53
	520	21185	3.12E8	3.07E-11	0.92	8.91E8	1.90E-9	0.73	2.01E8	5.53E-9	0.72	124.5
14 days	**NT**	6124	1.10E7	1.48E-10	0.84	6.96E6	3.09E-9	0.99	8.95E5	7.72E-7	0.61	83.99
	450	16893	5.94E6	5.18E-11	0.85	1.58E7	5.00E-11	0.90	1.54E7	3.19E-7	0.55	32.57
	480	5.61E7	3.39E7	1.05E-8	0.003	5.23E5	1.26E-10	0.99	1E20	1.63E-7	0.07	151.55
	520	18061	2.94E6	6.53E-11	0.86	1.58E6	6.14E-11	0.98	1.21E7	5.70E-7	0.38	86.19
21 days	**NT**	10077	1.2439E8	1.41E-10	0.84	9.5014E7	4.49E-13	0.99	1.11E7	1.21E-7	0.80	30.50
	450	31599	8.8381E9	8.88E-11	0.86	8.4918E9	9.36E-13	0.99	1.1E20	1.51E-6	0.25	37.67
	480	3505	1.6393E6	4.80E-11	0.92	1.1946E7	4.18E-11	0.95	5.08E6	6.278E-8	0.75	89.91
	520	79699	5.3641E8	7.44E-11	0.82	1.167E9	1.83E-8	0.99	1.3E9	9.44E-9	0.48	11.02

Source: The authors.

ordered or randomly distributed anionic voids [9]. In the Y-Zr-O-N samples, there are anionic voids due to the incorporation of yttria and nitrogen. The incorporation of nitrogen stabilizes the tetragonal structure, which generates remarkable improvements in the resistance to the hydrolytic degradation. Similarly, the properties of protection against degradation are influenced by the formation of amorphous oxides the presence of which is evidenced in the impedance spectra, in the analysis of atomic force microscopy, and in the SEM analysis. The stability of these oxides and their integration with the crystalline oxide structure of zirconia is favored with the presence of anionic voids in the 3Y-TZP structure

4. Conclusions

A significant effect on the increase of resistance to the degradation of 3Y-TZP zirconia with the incorporation of nitrogen by gaseous plasma was analyzed using electrochemical impedance spectroscopy, SEM-EDS microscopy, and AFM atomic force microscopy. 3Y-TZP samples without nitriding and nitrided at different temperatures showed similar hydrolytic degradation patterns, especially the formation of amorphous oxides. These were more stable in the nitriding samples, and they increased in the sample treated at 450 °C, which showed the highest resistance to degradation in artificial saliva. The nitriding processes induced stability in 3Y-TZP zirconia, which favors the electrochemical behavior of these materials that are used as a biomaterial in dental prostheses and bone implants.

Acknowledgements

The authors acknowledge the Sistema General de Regalías de Colombia (SGR) macroproyecto de Salud [BPIN code: 2012000100172] for funding this research.

References

[1] Chevalier, J. and Gremillard, L., 1.6 Zirconia as a biomaterial, in: Compr. Biomater. II, Elsevier, pp. 122-144, 2017. DOI: 10.1016/B978-0-12-803581-8.10245-0.

[2] Yin, L., Nakanishi, Y., Alao, A.R., Song, X.F, Abduo, J. and Zhang, Y., A review of engineered zirconia surfaces in biomedical applications, Procedia CIRP. 65, pp. 284-290, 2017. DOI: 10.1016/J.PROCIR.2017.04.057.

[3] Pieralli, S., Kohal, R.J., Lopez Hernandez, E., Doerken, S. and Spies, B.C., Osseointegration of zirconia dental implants in animal investigations: A systematic review and meta-analysis, Dent. Mater. 34, pp. 171-182, 2018. DOI: 10.1016/J.DENTAL.2017.10.008.

[4] Cattani-Lorente, M., Durual, S., Amez-Droz, M, Wiskott, H.W.A. and Scherrer, S.S., Hydrothermal degradation of a 3Y-TZP translucent dental ceramic: a comparison of numerical predictions with experimental data after 2 years of aging, Dent. Mater. 32, pp. 394-402, 2016. DOI: 10.1016/J.DENTAL.2015.12.015.

[5] Pandoleon, P., Kontonasaki, E., Kantiranis, N., Pliatsikas, N., Patsalas, P., Papadopoulou, L., Zorba, T., Paraskevopoulos, K.M. and Koidis, P., Aging of 3Y-TZP dental zirconia and yttrium depletion, Dent. Mater. 33, pp. e385-e392, 2017. DOI: 10.1016/J.DENTAL.2017.07.011.

[6] Bartolo, D., Cassar, G., Al-Haj Husain, N., Özcan, M. and Camilleri, J., Effect of polishing procedures and hydrothermal aging on wear characteristics and phase transformation of zirconium dioxide, J. Prosthet. Dent. 117, pp. 545-551, 2017. DOI: 10.1016/j.prosdent.2016.09.004.

[7] Sivaraman, K., Chopra, A., Narayan, A.I. and Balakrishnan, D., Is zirconia a viable alternative to titanium for oral implant? A critical review, J. Prosthodont. Res., 62(2), pp. 121-133, 2017. DOI: 10.1016/J.JPOR.2017.07.003.

[8] Abd El-Ghany, O.S. and Sherief, A.H., Zirconia based ceramics, some clinical and biological aspects: Review, Futur. Dent. J. 2, pp. 55-64, 2016. DOI: 10.1016/J.FDJ.2016.10.002.

[9] Berendts, S., Eufinger, J.P., Valov, I., Janek, J. and Lerch, M., Ionic conductivity of low yttria-doped cubic zirconium oxide nitride single crystals, Solid State Ionics. 296, pp. 42-46, 2016. DOI: 10.1016/J.SSI.2016.08.015.

[10] Liu, H., Zhao, W., Ji, Y., Cui, J., Chu, Y. and Rao, P., Determination of fracture toughness of zirconia ceramics with different yttria

concentrations by SEVNB method, Ceram. Int. 43, pp. 10572-10575, 2017. DOI: 10.1016/J.CERAMINT.2017.04.064.
[11] Almeida, P.J., Silva, C.L., Alves, J.L., Silva, F.S. and Martins, R.C., Sampaio-Fernandes, J., Analysis of the stability of 3Y-TZP zirconia abutments after thermocycling and mechanical loading, Rev. Port. Estomatol. Med. Dentária E Cir. Maxilofac. 57, pp. 197-206, 2016. DOI: 10.1016/J.RPEMD.2016.07.003.
[12] Cotič, J., Jevnikar, P. and Kocjan, A., Ageing kinetics and strength of airborne-particle abraded 3Y-TZP ceramics, Dent. Mater. 33, pp 847-856, 2017. DOI: 10.1016/J.DENTAL.2017.04.014.
[13] Cattani-Lorente, M., Scherrer, S.S., Durual, S, Sanon, C., Douillard, T., Gremillard, L., Chevalier, J. and Wiskott, A., Effect of different surface treatments on the hydrothermal degradation of a 3Y-TZP ceramic for dental implants, Dent. Mater. 30, pp. 1136-1146, 2014. DOI: 10.1016/j.dental.2014.07.004.
[14] Pajkossy, T. and Jurczakowski, R., Electrochemical impedance spectroscopy in interfacial studies, Curr. Opin. Electrochem. 1, pp. 53-58, 2017. DOI: 10.1016/J.COELEC.2017.01.006.
[15] Gan, K., Liu, H., Jiang, L., Liu, X., Song, X., Niu, D., Chen, T. and Liu, C., Bioactivity and antibacterial effect of nitrogen plasma immersion ion implantation on polyetheretherketone, Dent. Mater. 32, pp. e263-e274, 2016. DOI: 10.1016/J.DENTAL.2016.08.215.
[16] Romonti, D.E., Gomez-Sanchez, A.V., Milošev, I., Demetrescu, I. and Ceré, S., Effect of anodization on the surface characteristics and electrochemical behaviour of zirconium in artificial saliva, Mater. Sci. Eng. C. 62, pp. 458-466, 2016. DOI: 10.1016/j.msec.2016.01.079.
[17] Platt, P., Mella, R., DeMaio, W., Preuss, M. and Wenman, M.R., Peridynamic simulations of the tetragonal to monoclinic phase transformation in zirconium dioxide, Comput. Mater. Sci. 140, pp. 322-333, 2017. DOI: 10.1016/J.COMMATSCI.2017.09.001.
[18] Zhang, F., Batuk, M., Hadermann, J., Manfredi, G., Mariën, A., Vanmeensel, A., Inokoshi, M., Van Meerbeek, B., Naert, I. and Vleugels, J., Effect of cation dopant radius on the hydrothermal stability of tetragonal zirconia: Grain boundary segregation and oxygen vacancy annihilation, Acta Mater. 106, pp. 48-58, 2016. DOI: 10.1016/J.ACTAMAT.2015.12.051.
[19] Wei, C. and Gremillard, L., Towards the prediction of hydrothermal ageing of 3Y-TZP bioceramics from processing parameters, Acta Mater. 144, pp. 245-256, 2018. DOI: 10.1016/J.ACTAMAT.2017.10.061.
[20] Boccaccini, D.N., Frandsen, H.L, Soprani, S., Cannio, M., Klemensø, T., Gil, V. and Hendriksen, P.V., Influence of porosity on mechanical properties of tetragonal stabilized zirconia, J. Eur. Ceram. Soc. 38, pp. 1720-1735, 2018. DOI: 10.1016/J.JEURCERAMSOC.2017.09.029.
[21] Lee, J.S., Lerch, M. and Maier, J., Nitrogen-doped zirconia: A comparison with cation stabilized zirconia, J. Solid State Chem. 179, pp. 270-277, 2006. DOI: 10.1016/j.jssc.2005.10.012.
[22] Lee, J.S., Fleig, J., Maier, J., Chung, T.J. and Kim, D.Y., Microcontact impedance spectroscopy in nitrogen-graded zirconia, Solid State Ionics. 176, pp. 1711-1716, 2005. DOI: 10.1016/j.ssi.2005.04.036.

K. Dorado-Bustamante, was awarded his BSc. Eng. in Chemical Engineering in 2016 from the Universidad Nacional de Colombia, Medellin. The same year he was awarded a full scholarship from the Instituto Balseiro Patagonia, Argentina and currently, he is working in the department of nuclear physics in the Sp. degree of nuclear energy applications (CEATEN) in Buenos Aires, Argentina. His research interest includes: electrochemical processes, smart materials, and nuclear applications for biomedical devices.
ORCID: 0000-0002-2810-1191

S. Leal-Marin, was awarded her BSc. Eng. in Biomedical Engineering in 2013 from the Universidad EIA, Medellin, Colombia. For two years she worked for in the biomedical devices area, specifically in the neurological and orthopedic field. Currently, she works for the Universidad Nacional de Colombia, Medellin as a characterization devices technician in the laboratory of biomaterials, and she is undertaking a MSc. Eng. Materials and processes. Her research interests include the biological characterization of biomaterials, the development of coatings, and biomedical devices.
ORCID: 0000-0002-0315-1950

H. Estupiñán-Duran, was awarded his BSc. Eng. in Metallurgy Engineering in 2001, his MSc. Eng. in 2005, and his PhD. in Chemical Engineering in 2011, all them from the Universidad Industrial de Santander, Santander, Colombia. He then worked in the corrosion and development of biomaterials. Currently, he is a full professor in the Department of Materials and Minerals, Facultad de Minas, Universidad Nacional de Colombia, Medellin. His research interests include corrosion processes, surface characterization, biosensors, biocompatible and antibacterial coatings, and orthopedic materials.
ORCID: 000-0002-9607-3364